

# Enhanced antitumor effects by docetaxel/LL37-loaded thermosensitive hydrogel nanoparticles in peritoneal carcinomatosis of colorectal cancer

Rangrang Fan<sup>1,\*</sup>  
Aiping Tong<sup>1,\*</sup>  
Xiaoling Li<sup>1</sup>  
Xiang Gao<sup>1</sup>  
Lan Mei<sup>1</sup>  
Liangxue Zhou<sup>1</sup>  
Xiaoning Zhang<sup>2</sup>  
Chao You<sup>1</sup>  
Gang Guo<sup>1</sup>

<sup>1</sup>State Key Laboratory of Biotherapy and Cancer Center, Department of Neurosurgery, West China Hospital, Sichuan University, and Collaborative Innovation Center for Biotherapy, Chengdu, People's Republic of China;

<sup>2</sup>Department of Pharmacology and Pharmaceutical Sciences, School of Medicine, Tsinghua University, and Collaborative Innovation Center for Biotherapy, Beijing, People's Republic of China

\*These authors contributed equally to this work

Correspondence: Gang Guo; Liangxue Zhou

Department of Neurosurgery, State Key Laboratory of Biotherapy and Cancer Center, West China Hospital, Sichuan University, 17#, 3 Duan, Renmin Nan road, Chengdu, Sichuan 610041, People's Republic of China  
Tel +86 28 8516 4063  
Fax +86 28 8516 4060  
Email guogang@scu.edu.cn; liangxue\_zhou@126.com

**Abstract:** Intraperitoneal chemotherapy was explored in clinical trials as a promising strategy to improve the therapeutic effects of chemotherapy. In this work, we developed a biodegradable and injectable drug-delivery system by coencapsulation of docetaxel (Doc) and LL37 peptide polymeric nanoparticles (Doc+LL37 NPs) in a thermosensitive hydrogel system for colorectal peritoneal carcinoma therapy. Firstly, polylactic acid (PLA)-Pluronic L35-PLA (PLA-L35-PLA) was explored to prepare the biodegradable Doc+LL37 NPs using a water-in-oil-in-water double-emulsion solvent-evaporation method. Then, biodegradable and injectable thermosensitive PLA-L64-PLA hydrogel with lower sol-gel transition temperature at around body temperature was also prepared. Transmission electron microscopy revealed that the Doc+LL37 NPs formed with the PLA-L35-PLA copolymer were spherical. Fourier-transform infrared spectra certified that Doc and LL37 were encapsulated successfully. X-ray diffraction diagrams indicated that Doc was encapsulated amorphously. Intraperitoneal administration of Doc+LL37 NPs-hydrogel significantly suppressed the growth of HCT116 peritoneal carcinomatosis *in vivo* and prolonged the survival of tumor-bearing mice. Our results suggested that Doc+LL37 NPs-hydrogel may have potential clinical applications.

**Keywords:** intraperitoneal chemotherapy, injectable, nanoparticles, hydrogel, coencapsulation

## Introduction

Antimicrobial peptides, also known as host-defense peptides, exist in eukaryotic cells as a conserved component of the innate immune system. LL37, the only human cathelicidin, is formed from the last 37 amino acid residues of the C-terminus of human cationic antimicrobial peptide 18. Ren et al reported that LL37 is an endogenous tumor-suppressing peptide. They showed that the expression of LL37 was remarkably downregulated in human colon cancer tissues, whereas exogenous LL37 induced apoptotic cell death in cultured colon cancer cells.<sup>1,2</sup>

However, LL37 strongly reduced cell viability at high doses (20–60  $\mu\text{mol/L}$ ), and it did not show any effect at low doses (0.5–10  $\mu\text{mol/L}$ ) or even stimulate cell proliferation in other cancer types.<sup>1</sup> The combination of LL37 and an anticancer chemotherapy drug was considered to achieve higher antitumor efficacy and minimize the emergence of resistance. Docetaxel (Doc), a semisynthetic analog of paclitaxel, is a widely used anticancer agent that has been used for the treatment of various human malignancies.<sup>3–5</sup> Unlike single-agent therapy, the combination of several types of therapeutic approaches can modulate different signaling pathways in diseased cells, maximizing the therapeutic effect, and is considered to be a potential strategy for the effective treatment of cancers.<sup>3,6</sup> The combination of Doc with other bioactive agents has been widely studied.<sup>7–10</sup>

In this study, we tested the hypothesis that the combination of LL37 and Doc might enhance the antitumor activity of Doc for colorectal peritoneal carcinomatosis. The possible mechanism of action whereby LL37 enhances Doc therapeutic effect may be that its ability to disrupt the cell membrane could enhance the amount of Doc transported into colorectal peritoneal carcinomatosis HCT116 cells. These could improve the antiangiogenesis and antitumor activity of Doc.<sup>11–13</sup>

Systemic chemotherapy, a conventional treatment approach for patients with colorectal peritoneal carcinomatosis, usually provides a median survival of less than 12 months.<sup>14</sup> Also, traditional intravenous systemic chemotherapy has shown severe systemic toxicity, including immunosuppression, neurotoxicity, and myelosuppression. That toxicity remarkably limited the intensity of chemotherapy and lessened the life quality of patients.<sup>15–17</sup> Compared with an intravenous approach, intraperitoneal chemotherapy could expose tumors located in the peritoneal cavity to high drug concentrations while reducing systemic toxicity.<sup>18</sup> Intraperitoneal therapy has been proved to achieve higher peritoneal concentrations compared to plasma concentrations for 5-fluorouracil, doxorubicin, and paclitaxel.<sup>19,20</sup>

Thermosensitive hydrogels used for intraperitoneal therapy have been widely studied, due to their smart responsibility to the environmental stimulus and their biocompatibility.<sup>21</sup> Perfect thermosensitive hydrogels can flow freely at lower temperatures, but turn into gel at body temperature  $\sim 37^{\circ}\text{C}$ .<sup>22</sup> The delivery of anticancer drugs with thermosensitive hydrogels can prolong duration time and reduce systemic toxicity.<sup>23</sup> However, drugs loaded directly into hydrogels often result in relatively rapid drug release, due to the high water content and large pore sizes of hydrogels. The quantity and homogeneity of hydrophobic drug loading (DL) into hydrogels may be limited.<sup>24,25</sup> On the other hand, over the past decade, polymeric nanoparticles (NPs) made from natural and synthetic polymers have received the majority of attention and been employed as a drug-delivery system for cancer therapy.<sup>26–28</sup> NPs or micelles have shown rapid clearance from the peritoneal cavity.<sup>29</sup> Considering the advantages of polymeric thermosensitive hydrogels, in this study, Doc and LL37 were co-loaded in polylactic acid (PLA)-Pluronic L35-PLA (PLA-L35-PLA) NPs (Doc+LL37 NPs), and then the Doc+LL37 NPs were dispersed in PLA-L64-PLA (number-average molecular weight [ $M_n$ ] 4,500) thermosensitive hydrogel to prepare Doc+LL37 NPs–hydrogel composites, and treatment with Doc+LL37 NPs–hydrogel composites in colorectal peritoneal carcinomatosis HCT116 models was evaluated. Our

findings indicated that the NP–hydrogel composites improved antiangiogenesis and antitumor activity both in vitro and in vivo, and might have great potential clinical application.

## Materials and methods

### Materials, cell lines, and animals

D,L-Lactide was obtained from Jinan Daigang Biomaterial Co Ltd (Jinan, People's Republic of China). L35 ( $M_n$  1,900), L64 ( $M_n$  2900), stannous octanoate ( $\text{Sn}[\text{Oct}]_2$ ), polyvinyl alcohol (PVA; weight-average molecular weight 30,000–70,000, hydrolysis degree 87%–90%) and MTT were obtained from Sigma-Aldrich Co (St Louis, MO, USA). Doc was provided by Sichuan Xieli Pharmaceutical Co Ltd (Chengdu, People's Republic of China). LL37 (95.0% pure) was purchased from Shanghai Aobo Pharmtech Inc Ltd (Shanghai, People's Republic of China). All other agents – methylbenzene, petroleum ether, dichloromethane, tetrahydrofuran, and glycerol – were of analytical reagent grade and used as received from the manufacturer.

HCT116 and HEK293 cells were purchased from the American Type Culture Collection (Manassas, VA, USA) and grown in Roswell Park Memorial Institute 1640 medium supplement with 10% fetal bovine serum (FBS; Thermo Fisher Scientific, Waltham, MA, USA). The cell culture was maintained in a  $37^{\circ}\text{C}$  incubator with a humidified 5%  $\text{CO}_2$  atmosphere.

BALB/c nude mice (6–8 weeks) were purchased from the Animal Center Laboratory of Beijing HFK Bioscience Co Ltd (Beijing, People's Republic of China). The animals were housed in a controlled temperature of  $20^{\circ}\text{C}$ – $22^{\circ}\text{C}$ , with relative humidity of 50%–60% and 12-hour light–dark cycles. The animals were provided with standard laboratory chow and tap water ad libitum. All animal procedures were performed following the protocol approved by the Institutional Animal Care and Treatment Committee of Sichuan University (Chengdu, People's Republic of China). All mice were treated humanely throughout the experimental period, and the study was approved by the ethics committee of Sichuan University.

### Synthesis of PLA-L35-PLA and PLA-L64-PLA block copolymers

PLA-L35-PLA biodegradable block copolymers were synthesized by ring-opening polymerization. Briefly, a known amount of D,L-lactide and L35 were introduced into a dry glass ampoule under a nitrogen atmosphere, and 0.3% of  $\text{Sn}(\text{Oct})_2$  were added. The ampoule was kept at  $130^{\circ}\text{C}$ . During polymerization, the system was stirred slowly, and viscosity increased over time. Ten hours later, the system was

rapidly heated to 150°C under vacuum for an additional hour. After being cooled to room temperature under a nitrogen atmosphere, the PLA-L35-PLA copolymer was first dissolved in methylene chloride and reprecipitated from the filtrate using excess cold petroleum ether. The mixture was filtered and dried to a constant weight at 40°C in vacuum. PLA-L64-PLA block copolymers were synthesized in a similar manner. Then, the obtained purified PLA-L35-PLA and PLA-L64-PLA copolymers were kept in airtight bags in desiccators before use.

<sup>1</sup>H-nuclear magnetic resonance (NMR) spectroscopy was recorded on an Avance III 400 (Bruker Optik GmbH, Ettlingen, Germany) at 400 MHz using deuterated chloroform (CDCl<sub>3</sub>) as the solvent and tetramethylsilane as the internal reference standard. Gel permeation chromatography (GPC; Agilent 110 high-performance liquid chromatography [HPLC]; Agilent Technologies, Santa Clara, CA, USA) was used to determine the macromolecular weight and macromolecular weight distribution of PLA-L35-PLA and PLA-L64-PLA copolymers.

## Preparation and characterization of Doc+LL37 NPs

The water-in-oil-in-water (w/o/w) double-emulsion-solvent evaporation method was used to prepare the Doc+LL37 NPs. Briefly, 9.5 mg of PLA-L35-PLA ( $M_n$  1.0×10<sup>4</sup>, 2.0×10<sup>4</sup>, and 3.0×10<sup>4</sup>, respectively) and 0.5 mg Doc were dissolved in 1 mL of dichloromethane ethyl acetate (1/1, v/v) as the organic phase. Then, the organic phase was emulsified with a mixture of 100 μL of LL37 solution (10 mg/mL) by probe sonication at a certain amplitude for 60 seconds in an ice bath (TM300 sonic disruptor; Teledyne Tekmar, Mason, OH, USA). The primary emulsion was added dropwise to 4 mL of 1% (w/v) PVA solution, and the mixture was sonicated for 60 seconds followed by rotary evaporation under vacuum to remove the organic solvents at 37°C (Rotavapor® R-114; Büchi, Flawil, Switzerland). The prepared Doc+LL37 NPs were finally collected by centrifugation at 13,300 rpm at 4°C for 90 minutes (Eppendorf, Hamburg, Germany). The supernatant was used for determination of the unencapsulated LL37. Doc-loaded NPs were prepared as mentioned earlier, except for the addition of LL37. Blank NPs were prepared as mentioned earlier, except for the addition of LL37 and Doc during the formulation preparation. All the particles were then lyophilized (Labconco, Kansas City, MO, USA) and stored at 4°C until further use.

The particle-size distribution, polydispersity index (PDI), and zeta potential of prepared blank NPs and Doc+LL37 NPs

were determined by a Malvern Nano ZS 90 laser particle-size analyzer at 25°C. All results are the mean of three test runs, and all data are expressed as mean ± standard deviation.

Encapsulation efficiency (EE) was calculated by dividing the LL37 or Doc amount in the particle fraction by the amount of LL37 or Doc added initially. The amount of LL37 in the particle fraction was indirectly calculated by subtracting the amount of unencapsulated LL37 in the supernatant from the amount of LL37 added initially. The amount of LL37 was quantified by HPLC (Alliance 2695; Waters, Milford, MA, USA). The analysis of Doc was carried out at room temperature with an Apollo C18 column (150×4.6 mm, 5 μL; WR Grace and Company, Columbia, MD, USA) at 230 nm for Doc. Mixtures of acetonitrile and ultrapure water (48:52, v/v) were used as the mobile phase, and the flow rate was 1.0 mL/min. Briefly, exactly weight-lyophilized NPs were dissolved in dimethyl sulfoxide, and the resulting solutions were properly diluted prior to HPLC analysis. The amount of Doc in the NPs was determined from the peak area correlated with the standard curve. All analyses were performed in triplicate.

The morphological characteristics of Doc+LL37 NPs were examined by transmission electron microscopy (TEM; H-6009IV; Hitachi Ltd, Tokyo, Japan). NPs were diluted with distilled water and placed on a copper grid covered with nitrocellulose. Samples were negatively stained with phosphotungstic acid and dried at room temperature.

## Preparation and characterization of Doc+LL37 NPs–hydrogel composites

To prepare Doc+LL37 NPs–hydrogel composites, PLA-L64-PLA copolymer ( $M_n$  4,500) was well dissolved in water at 60°C and then cooled to 4°C to form sol. Then, the premade NPs were mixed with PLA-L64-PLA hydrogel to form a homogeneous solution, and the concentration of PLA-L64-PLA hydrogel was kept at 20 wt%. Scanning electron microscopy (SEM; JSM-5900LV; JEOL, Tokyo, Japan) was employed to investigate the morphology of PLA-L64-PLA hydrogel, and samples were frozen in liquid nitrogen and lyophilized for 36 hours. Then, the samples were sputtered with gold before observation.

Sol–gel–sol transition of PLA-L64-PLA hydrogel was investigated by rheometry (Haake RheoStress 6000; Thermo Fisher Scientific). Calculated amounts of PLA-L64-PLA copolymers were dissolved in deionized water at a designated temperature to obtain the copolymer aqueous solution. The aqueous PLA-L64-PLA copolymer solution was placed between parallel plates of 40 mm diameter and

a gap of 31  $\mu\text{m}$ . Data were collected under controlled stress (0.5 dyn/cm<sup>2</sup>) and a frequency of 1.0 rad/s. The heating rate was 1°C/min in the range of 15°C–60°C.

## X-ray diffraction assay

The crystalline states of samples were analyzed on an X'Pert Pro MPD DY1291 (Philips, Amsterdam, the Netherlands) diffractometer using graphite-monochromatized CuK radiation ( $\lambda=0.1542$  nm; 40 kV; 40 mA) at a scanning rate of 4°/min.

## In vitro release study

In vitro release of Doc from Doc NPs and Doc NPs–hydrogel was carried out in 1 mL of phosphate-buffered saline (PBS; 0.01 M, pH 7.4) containing 0.5% v/v Tween 80 (to maintain a sink condition) and was placed in a dialysis tube (molecular weight cutoff 3,500–7,000). The dialysis tubes were placed in bottles with 10 mL PBS (pH 7.4, temperature 37°C) containing Tween 80 (0.5% v/v) or PBS solution containing 10% FBS in an incubator at 37°C and kept in a shaker at 120 rpm. At specific time intervals, all medium was withdrawn and replaced with an equivalent volume of fresh PBS solution. The concentration of Doc released from hydrogel was determined via HPLC. Three independent experiments were carried out, and the averaged values are used in data presentation.

## In vitro cytotoxicity against HCT116 cells

The cytotoxicity of free Doc, free LL37, and free Doc+LL37 on HCT116 cells was evaluated using an MTT colorimetric procedure. Briefly, HCT116 cells were plated at a density of  $3 \times 10^3$  cells per well in 96-well plates and grown for 24 hours. Then, cells were exposed to a series of free Doc, free LL37, and free Doc+LL37 at different concentrations for 48 hours. The viability of cells was measured using MTT. Data are expressed as the percentages of viable cells compared to the survival of the control group, and all data are expressed as mean  $\pm$  standard deviation.

The combination index (CI) was used to analyze the synergistically inhibitory effect of drug combinations.<sup>30</sup> CI < 1 represents synergistic cytotoxicity, CI = 1 represents additive cytotoxicity, and CI > 1 represents antagonistic cytotoxicity.<sup>31</sup>

## Cell-apoptosis assay

HCT116 cells ( $5 \times 10^5$ ) were grown on coverslips placed into six-well plates and allowed to attach overnight, treated with 20  $\mu\text{g}$  LL37, 2  $\mu\text{g}$  Doc, or a combination thereof for 24 hours. Cells were fixed with cold methanol and acetic acid (3/1, v/v) at 4°C overnight and stained with terminal

deoxynucleotidyl transferase deoxyuridine triphosphate nick-end labeling (TUNEL) for 30 minutes in the dark, washed again in PBS, and finally mounted in mounting medium (80% glycerol in PBS). Processed cells were observed with a fluorescence microscope (DM2500; Leica Microsystems, Wetzlar, Germany).

## In vivo tumor model and treatment plan

The antitumor effect of Doc+LL37 NPs–hydrogel was evaluated using a colorectal peritoneal carcinomatosis mouse model. The BALB/c nude mice were intraperitoneally injected with 200  $\mu\text{L}$  of cell suspension containing  $5 \times 10^6$  HCT116 cells. Tumors were allowed to grow for 10 days. Then, tumor-bearing mice were randomly assigned to one of the following six groups (12 mice per group): normal saline (NS), blank NPs–hydrogel, free Doc, Doc NPs–hydrogel, free (Doc+LL37) and Doc+LL37 NPs–hydrogel. Treatments were administered through intraperitoneal injection with a single dose of 200  $\mu\text{L}$  of the aforementioned. Free Doc and free Doc+LL37 solution were used as a single injection at a Doc dose of 8 mg/kg, and Doc NPs–hydrogel and Doc+LL37 NPs–hydrogel solution were used as a single injection at a dose of 16 mg Doc/kg. The free drug group was treated twice a week, and the Doc NPs–hydrogel and Doc+LL37 NPs–hydrogel group was given drug once a week.

For tumor-inhibition study (six mice per group), the number and weight of tumor nodules were measured on day 30, and tumor tissues were collected for immunofluorescent analysis. After day 24, mice in the NS group began to die. To study further the therapeutic effect against colorectal cancer, the survival time of mice treated with the protocols described was observed (ten mice per group).

## Immunohistochemical determination of CD31

The tumors were stored at  $-80^\circ\text{C}$  to examine microvessel expression, then frozen sections of tumors were cut at 8–10  $\mu\text{m}$  thickness using a cryostat (Leica Microsystems), fixed in acetone, and washed with PBS. After permeabilization (Triton X-100 0.1% v/v in PBS; Sigma-Aldrich) and blocking (5% w/v bovine serum albumin in PBS), the primary antibody (rat anti-CD-31 [1:50]; Pharmingen™; BD Biosciences, San Jose, CA, USA) was applied for 1 hour at 37°C, followed by incubation with a fluorescein isothiocyanate-conjugated secondary antibody (Abcam PLC, Cambridge, UK). Finally, sections were incubated with 4',6-diamidino-2-phenylindole (50 ng/mL; Thermo Fisher Scientific) for 5 minutes to visualize the cell nuclei. Microvessel density (MVD) was calculated as the average number of small

CD31-positive vessels in a high-power (400×) field using a fluorescence microscope (DM2500; Leica Microsystems).

## Statistical analysis

Statistical analysis was carried out using SPSS 15.0 software (SPSS Inc, Chicago, IL, USA). Comparisons of tumor-nodule number and tumor weight were performed using one-way analysis of variance. Survival curves were generated by the Kaplan–Meier method, and the log-rank test was used to compare the distributions of survival times. All reported *P*-values are two-sided, and were considered to be statistically significant at  $P < 0.05$ ,  $P < 0.01$ , and  $P < 0.001$ .

## Results

### Characterization of PLA-L35-PLA

A series of PLA-L35-PLA biodegradable block copolymers was synthesized by ring-opening polymerization, and then was used to prepare Doc+LL37 NPs as shown in Figure 1. Figure 2A showed the <sup>1</sup>H-NMR curves of PLA-L35-PLA block copolymers. The molecular weight of the prepared PLA-L35-PLA block copolymers were  $M_n$  1.0×10<sup>4</sup> (10 k), 2.0×10<sup>4</sup> (20 k), and 3.0×10<sup>4</sup> (30 k), which were determined by GPC (Figure 2B). The molecular weight of prepared PLA-L35-PLA triblock copolymers were also calculated from

**Table 1** The PLA-L35-PLA copolymer obtained in this paper

Samples	$M_n^a$ (×10 <sup>4</sup> )	$M_n^b$ (×10 <sup>4</sup> )	Molecular weight		
			$M_w^c$ (×10 <sup>4</sup> )	$M_n^c$ (×10 <sup>4</sup> )	$M_w/M_n$
1	1.00	0.98	1.52	0.83	1.83
2	2.00	1.92	2.55	1.86	1.37
3	3.00	2.86	3.61	2.26	1.60

**Notes:** <sup>a</sup>Calculated from feed ratio; <sup>b</sup>determined by <sup>1</sup>H-NMR; <sup>c</sup>determined by GPC in tetrahydrofuran (polystyrene standard).

**Abbreviations:** PLA, polylactic acid;  $M_n$ , number-average molecular weight;  $M_w$ , weight-average molecular weight; NMR, nuclear magnetic resonance; GPC, gel permeation chromatography.

<sup>1</sup>H-NMR spectra (Figure S1). The data are summarized in Table 1. According to Table 1, the number-average molecular weight ( $M_n$ ) estimated from <sup>1</sup>H-NMR spectra was consistent with the theoretical value calculated from feed ratio.

### Preparation and characterization of Doc+LL37 NPs

As shown schematically in Figure 1, Doc+LL37 NPs were prepared by a w/o/w double-emulsion solvent-evaporation method. Figure 3A showed the photograph of different prepared NPs. The effects of Doc:copolymer ratios and LL37:copolymer ratios on the properties of the NPs were investigated in detail, and the results are exhibited in Table 2. The DL, EE, and particle size of a series of Doc NPs and

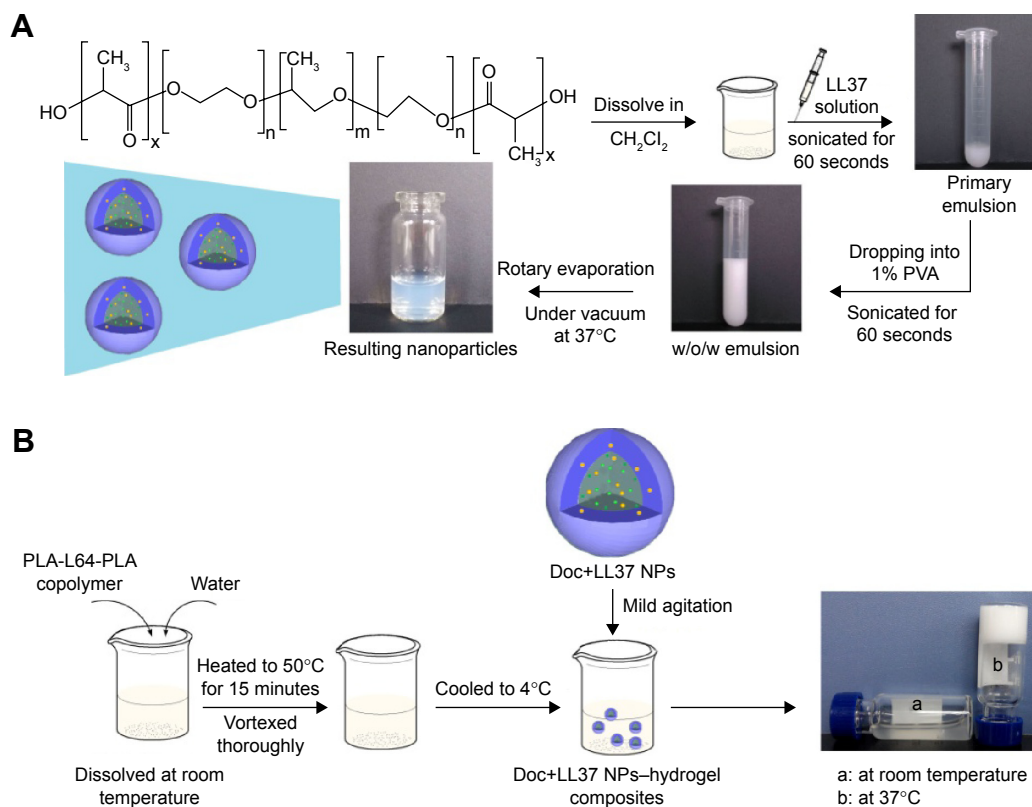


**Figure 1** Preparation schemes of NPs and NPs–hydrogel composite.

**Notes:** (A) Preparation scheme of Doc+LL37 NPs; (B) schematic representation of the Doc+LL37 NPs–hydrogel composite preparation.

**Abbreviations:** Doc, docetaxel; NPs, nanoparticles; PVA, polyvinyl alcohol; PLA, polylactic acid.

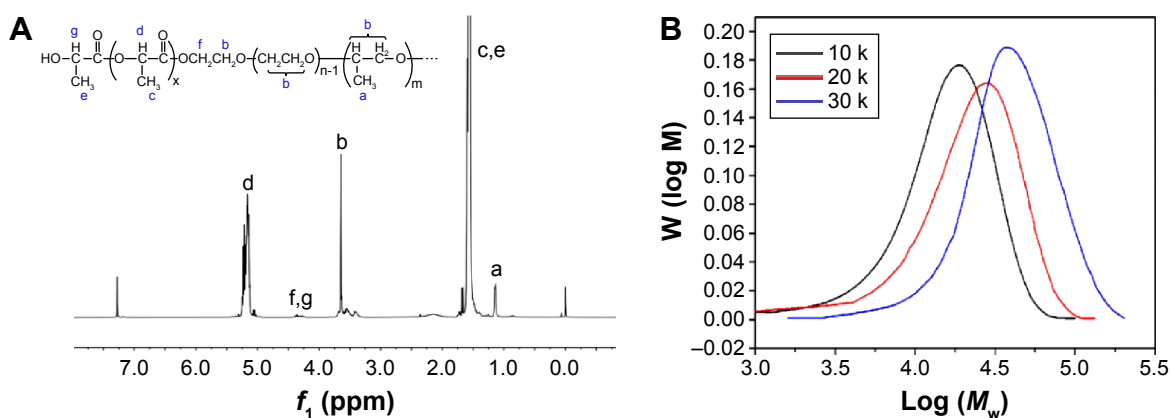


**Figure 2**  $^1\text{H-NMR}$  and GPC analysis.

**Notes:**  $^1\text{H-NMR}$  curves (A) and GPC curves (B) of PLA-L35-PLA block copolymers.

**Abbreviations:**  $^1\text{H-NMR}$ , hydrogen nuclear magnetic resonance; GPC, gel permeation chromatography; PLA, polylactic acid; W, weight.

Doc+LL37 NPs are shown in Table 2. With increased drug:copolymer ratio in feed, DL and particle size increased, whereas the EE decreased accordingly.

In consideration of DL and stability, S3 was chosen for further applications and was characterized in detail. The DL and EE of Doc were  $4.48\% \pm 0.34\%$  and  $89.65\% \pm 2.43\%$ , and of LL37  $7.49\% \pm 0.59\%$  and  $75.12\% \pm 2.57\%$ , respectively. In addition, as shown in Figure 3C, 3D and Table S1 the average particle size, PDI, and zeta potential of S3 were  $129.21 \pm 0.73$  nm,  $0.125 \pm 0.027$ , and  $2.37 \pm 0.08$ , respectively. The PDI and zeta potential of blank NPs and S1–S3 are listed in Table S1. According to the particle-size distribution spectra shown in Figure S2, the prepared NPs were monodisperse and had a very narrow particle-size distribution. In Figure 3B, the TEM image also revealed that Doc+LL37 NPs were monodisperse. In addition, the diameter of the polymeric Doc+LL37 NPs observed by TEM was in good agreement with the results of particle-size analysis. The microstructure of Doc+LL37 NPs observed by TEM, as well as the particle-size analysis, demonstrated that the prepared Doc+LL37 NPs were stable and were able to be well dispersed in aqueous solution.

Fourier-transform infrared spectra of free Doc (a), free LL37 (b), Doc NPs (c), Doc+LL37 NPs (d), and blank NPs (e) are shown in Figure 4A. The new bands of Doc+LL37 NPs at approximately  $750\text{ cm}^{-1}$ ,  $800\text{ cm}^{-1}$ , and  $1,700\text{ cm}^{-1}$

compared to the spectra of blank NPs certified that Doc and LL37 were encapsulated successfully.

Figure 4B presents the X-ray diffraction (XRD) patterns of free Doc, free LL37, Doc NPs, Doc+LL37 NPs, and blank NPs. Pure Doc is crystalline, with characteristic peaks at  $2\theta = 8.12^\circ, 9.32^\circ, 11.42^\circ, 12.62^\circ, 13.94^\circ, 16.94^\circ,$  and  $20.42^\circ$ . Pure LL37 is noncrystalline. Based on the XRD diagrams of free Doc, the absence of specific diffraction peaks in the Doc+LL37 NPs diagram indicated that Doc was encapsulated amorphously.

## Preparation and characterization of Doc+LL37 NPs–hydrogel composites

Figure 5A shows changes in the storage modulus ( $G'$ ) and loss modulus ( $G''$ ) for PLA-L64-PLA solution. It can be seen that the  $G'$  in sol state was less than 1 Pa and then increased abruptly due to the sol–gel transition as the temperature increased. The dramatic decrease in the  $G'$  at approximately  $41^\circ\text{C}$  demonstrates the gel–sol transition of the aqueous copolymer solution. The interior morphology of PLA-L64-PLA hydrogel was investigated by SEM. According to Figure 5B, the hydrogel shows a porous three-dimensional structure, and the micropores are approximately spherical with homogeneous mesh size, which enabled drug molecules to diffuse out of them.

The in vitro release profile of Doc from Doc NPs and Doc+LL37 NPs in PBS solution at pH 7.4 or 10% FBS is

**Table 2** Characterization of Doc+LL37 NPs prepared from PLA-L35-PLA

Sample	LL37/polymer (Doc 5%)	DL (%) of Doc	DL (%) of LL37	EE (%) of Doc	EE (%) of LL37	Size (nm)
S1	2.5%	$4.62 \pm 0.27$	$2.03 \pm 0.47$	$92.45 \pm 2.11$	$81.26 \pm 4.57$	$104.32 \pm 0.66$
S2	5%	$4.53 \pm 0.28$	$3.79 \pm 0.34$	$90.62 \pm 1.68$	$75.82 \pm 2.94$	$117.16 \pm 0.57$
S3	10%	$4.48 \pm 0.34$	$7.49 \pm 0.59$	$89.65 \pm 2.43$	$75.12 \pm 2.57$	$129.21 \pm 0.73$
S4	15%	$4.32 \pm 0.52$	$9.48 \pm 0.59$	$86.41 \pm 2.37$	$63.21 \pm 3.59$	$139.97 \pm 3.26$

**Abbreviations:** Doc, docetaxel; NPs, nanoparticles; PLA, polylactic acid; DL, drug loading; EE, encapsulation efficiency.

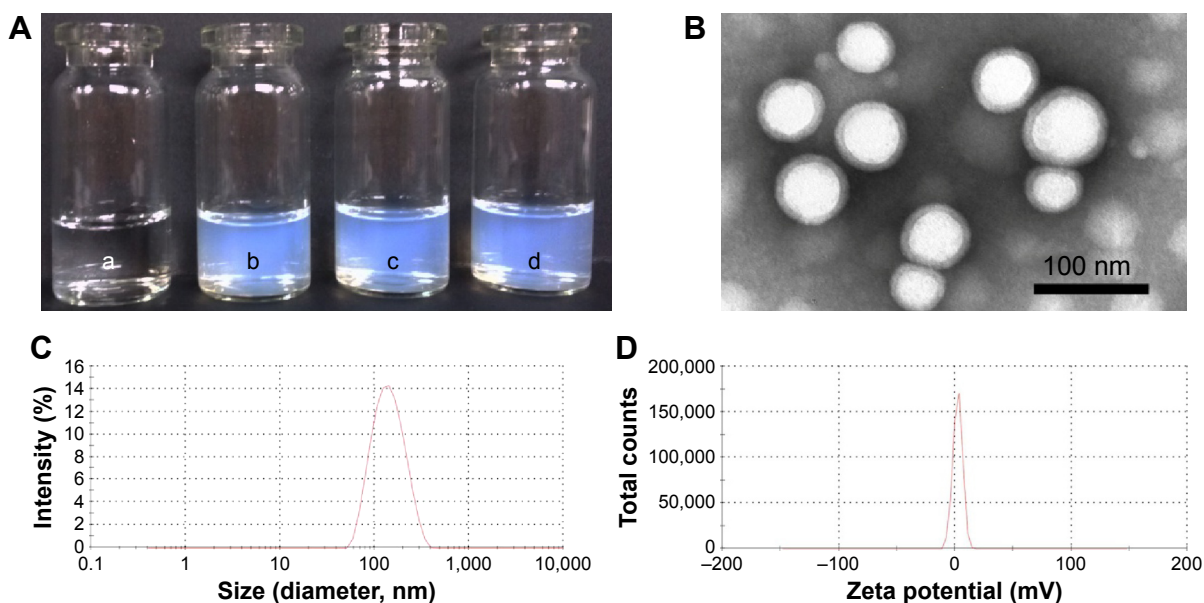


**Figure 3** Characterization of Doc+LL37 NPs.

**Notes:** (A) Photograph of water (a), blank NPs (b), Doc NPs (c), and Doc+LL37 NPs (d); (B) TEM image of Doc+LL37 NPs; (C) particle-size distribution of Doc 5%+LL37 10% NPs; (D) zeta potential of Doc 5%+LL37 10% NPs.

**Abbreviations:** Doc, docetaxel; NPs, nanoparticles; TEM, transmission electron microscopy.

presented in Figure 5C and D. The release rate of Doc from Doc NPs and Doc+LL37 NPs in PBS solution at pH 7.4 (no serum) was slower than that in PBS containing 10% FBS; however, the cumulative release of Doc on the 21st day between PBS solution at pH 7.4 and PBS containing 10% FBS showed no significant difference.

### Cytotoxicity and apoptosis analysis

The toxicity of free Doc, free LL37, and free Doc+LL37 was evaluated using MTT assay. MTT assay (Figure 6) showed that LL37 strongly reduced cell viability at high doses. LL37 did not show any effect on the viability of HCT116

at low doses. Free Doc+LL37 at various concentrations of Doc significantly decreased the viability of HCT116 cells in a dose-dependent manner. This suggested that Doc in combination with LL37 could achieve higher antitumor efficacy.

The LL37 and Doc concentrations to inhibit HCT116 proliferation when used alone or in association are listed in Table 3. As shown, the presence of both agents and doses of LL37 and Doc required to achieve inhibition of 30%, 50%, 70%, and 90% of HCT116 proliferation were considerably reduced. The combination of Doc and LL37 demonstrated an additive effect ( $CI > 1$ ) to produce 10%

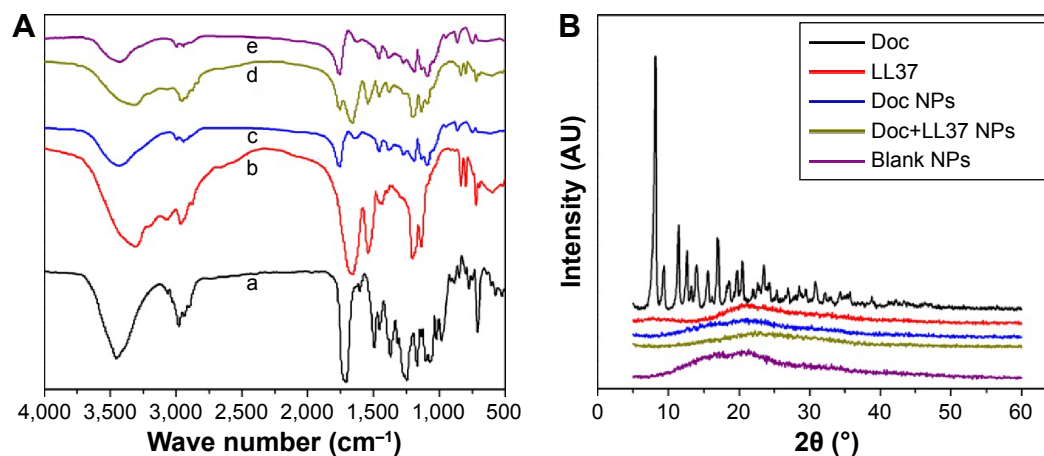


**Figure 4** FTIR and XRD analysis.

**Notes:** (A) FTIR spectra for free Doc (a), free LL37 (b), Doc NPs (c), Doc+LL37 NPs (d), and blank NPs (e); (B) XRD patterns of free Doc, free LL37, Doc NPs, Doc+LL37 NPs, and blank NPs.

**Abbreviations:** FTIR, Fourier-transform infrared spectroscopy; Doc, docetaxel; NPs, nanoparticles; XRD, X-ray diffraction.

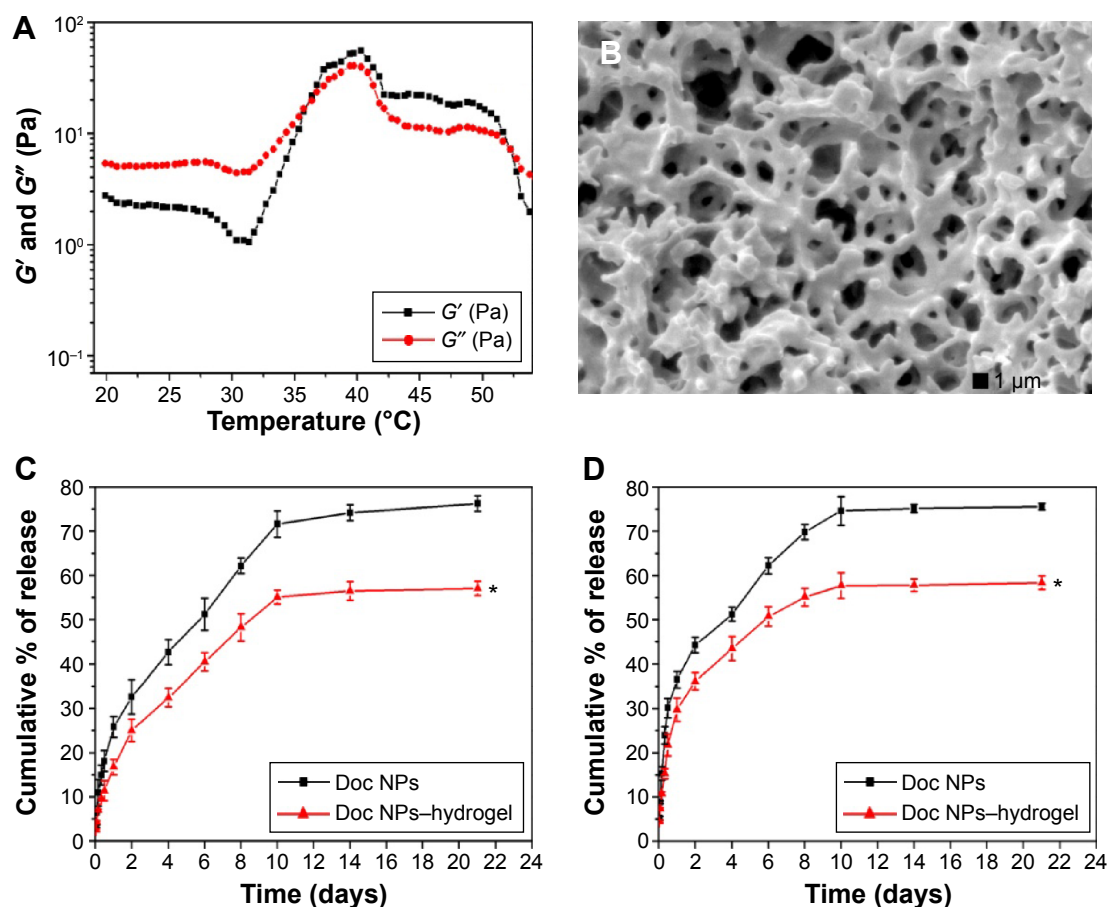


**Figure 5** The characterization of PLA-L64-PLA hydrogel and the in vitro release behavior.

**Notes:** (A) Rheology analysis of PLA-L64-PLA hydrogel as a function of temperature; (B) SEM image of PLA-L64-PLA hydrogel. In vitro release behavior of Doc from Doc NPs and Doc NPs-hydrogel in PBS solution at pH 7.4 (C) or 10% FBS (D). Data shown as mean  $\pm$  standard deviation ( $n=3$ ), and  $P<0.05$  on a two-tailed test was considered statistically significant. \* $P<0.05$  compared to the Doc NPs group.

**Abbreviations:**  $G'$ , storage modulus;  $G''$ , loss modulus; PLA, polylactic acid; SEM, scanning electron microscopy; Doc, docetaxel; NPs, nanoparticles; PBS, phosphate-buffered saline; FBS, fetal bovine serum.

inhibition of HCT116 proliferation and synergism ( $CI < 1$ ), to achieve 30%, 50%, 70%, and 90% inhibition of HCT116 proliferation.

As shown in Figure 7, the apoptogenic effect of free Doc, free LL37, and free Doc+LL37 in HCT116 colon cancer cells was subsequently confirmed by TUNEL assay. The combination group was more effective than the Doc- or LL37-alone groups, indicating that Doc was able to act synergistically with LL37 in vitro.

### In vivo antitumor activity

The ability of Doc+LL37 NPs-hydrogel composites to inhibit growth of HCT116 carcinoma in vivo was evaluated in a mouse model. As shown in Figure 8, the abdominal cavity images showed that the tumor-node numbers from the Doc+LL37 NPs-hydrogel-treated group were significantly lower than those of the other groups. Furthermore, the size of the tumor nodes was significantly smaller than those of the other groups. The mean number and weight of tumor nodules

in Doc+LL37 NPs-hydrogel group ( $18.21 \pm 1.92$ ,  $0.61 \pm 0.19$  g) were dramatically decreased compared with that in the free Doc+LL37 ( $26.62 \pm 4.72$ ,  $P < 0.01$ ;  $1.11 \pm 0.10$  g,  $P < 0.01$ ), Doc NPs-hydrogel ( $42.03 \pm 6.36$ ,  $P < 0.01$ ;  $1.66 \pm 0.16$  g,  $P < 0.01$ ), free Doc ( $48.04 \pm 7.18$ ,  $P < 0.01$ ;  $1.88 \pm 0.16$  g,  $P < 0.01$ ), NPs-hydrogel ( $75.13 \pm 4.64$ ,  $P < 0.01$ ;  $3.13 \pm 0.30$  g,  $P < 0.01$ ), or NS ( $73.62 \pm 8.68$ ,  $P < 0.01$ ;  $3.07 \pm 0.39$  g,  $P < 0.01$ ) groups. In addition, there was a significant increase in the life span of the Doc+LL37 NPs-hydrogel-treated mice: the median survival time in the Doc+LL37 NPs-hydrogel group (60 days) was significantly longer than that in the free Doc+LL37 (49 days,  $P < 0.01$ ), Doc NPs-hydrogel (48 days,  $P < 0.01$ ), free Doc (45 days,  $P < 0.01$ ), blank NPs-hydrogel (35 days,  $P < 0.01$ ), and NS (29 days,  $P < 0.01$ ) groups, respectively.

Sections of tumors from mice in each group were stained for CD31 immunofluorescence to determine MVD as a measurement of tumor angiogenesis. The Doc+LL37 NPs-hydrogel treatment resulted in dramatic inhibition of

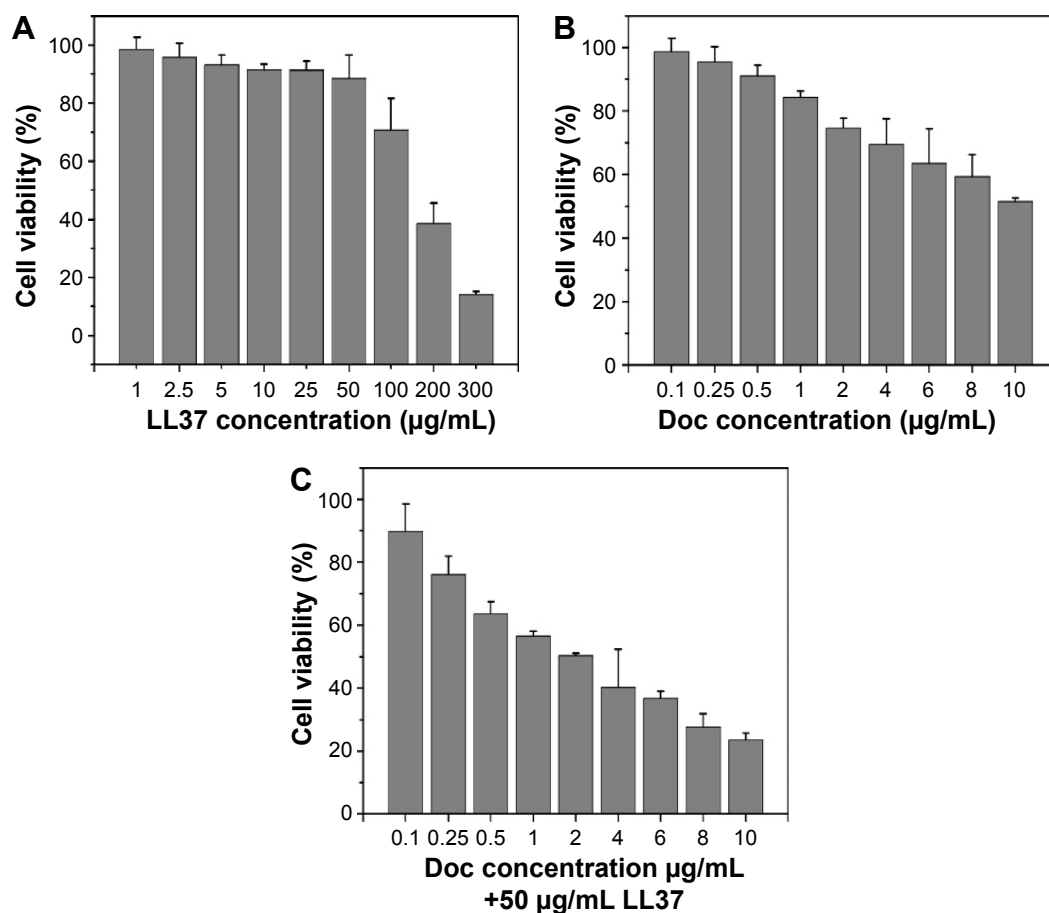


**Figure 6** Cytotoxicity studies of free LL37 (A), Doc (B) and Doc+LL37 (C).  
**Abbreviation:** Doc, docetaxel.

angiogenesis in the tumors (Figure 9). MVD in the Doc+LL37 NPs–hydrogel group was  $19.67 \pm 3.98$ , which was dramatically lower than that in the free Doc+LL37 group ( $33.00 \pm 7.40$ ,  $P < 0.01$ ), Doc NPs–hydrogel group ( $60.00 \pm 11.01$ ,  $P < 0.01$ ), free Doc group ( $65.50 \pm 7.37$ ,  $P < 0.01$ ), blank NPs–hydrogel group ( $112.00 \pm 17.32$ ,  $P < 0.01$ ), and NS ( $115.33 \pm 13.45$ ,  $P < 0.01$ ) group. The results implied that antiangiogenesis might be another mechanism of inhibiting colon cancer by Doc+LL37 NPs–hydrogel in vivo.

**Table 3** Doses necessary to inhibit HCT116 proliferation in an MTT assay by 10% (ID<sub>10</sub>), 30% (ID<sub>30</sub>), 50% (ID<sub>50</sub>), 70% (ID<sub>70</sub>), and 90% (ID<sub>90</sub>) by single-agent docetaxel or LL37 and by combination of docetaxel and LL37

	Docetaxel (µg/mL)	LL37 (µg/mL)	Docetaxel–LL37 (µg/mL)	CI
ID <sub>10</sub>	0.6	70	0.2/50	1.05
ID <sub>30</sub>	2	120	0.9/50	0.86
ID <sub>50</sub>	10	150	3/50	0.63
ID <sub>70</sub>	20	260	8/50	0.59
ID <sub>90</sub>	45	400	15/50	0.49

**Abbreviation:** CI, combination index.

## Discussion

Colorectal cancer is one of the leading cancer types, and accounts for approximately 10% of new cancer cases.<sup>32</sup> Chemotherapy is widely used in the clinic and has proved to be effective. Coencapsulation of multiple drugs into nanocapsules may play prominent roles in the treatment of cancers to achieve higher antitumor efficacy and minimize the emergence of resistance.<sup>33,34</sup> LL37, originally found in the innate immune system, is a robust antimicrobial peptide. It plays an important role in the maintenance of natural immunity, and has a direct effect on wound healing, neovascularization, and angiogenesis.<sup>35</sup> Chuang et al investigated whether LL37 could enhance the immunostimulatory effects of CpG oligodeoxynucleotides by increasing uptake into immune cells, thus enhancing the antitumor effects.<sup>36</sup> They found that treatment with the combination of CpG oligodeoxynucleotides and LL37 generated significantly better therapeutic antitumor effects and enhanced survival in tumor-bearing mice. Other researchers found LL37 could enhance adaptive immune response against macrophage colony-stimulating factor receptor cloned from the J61

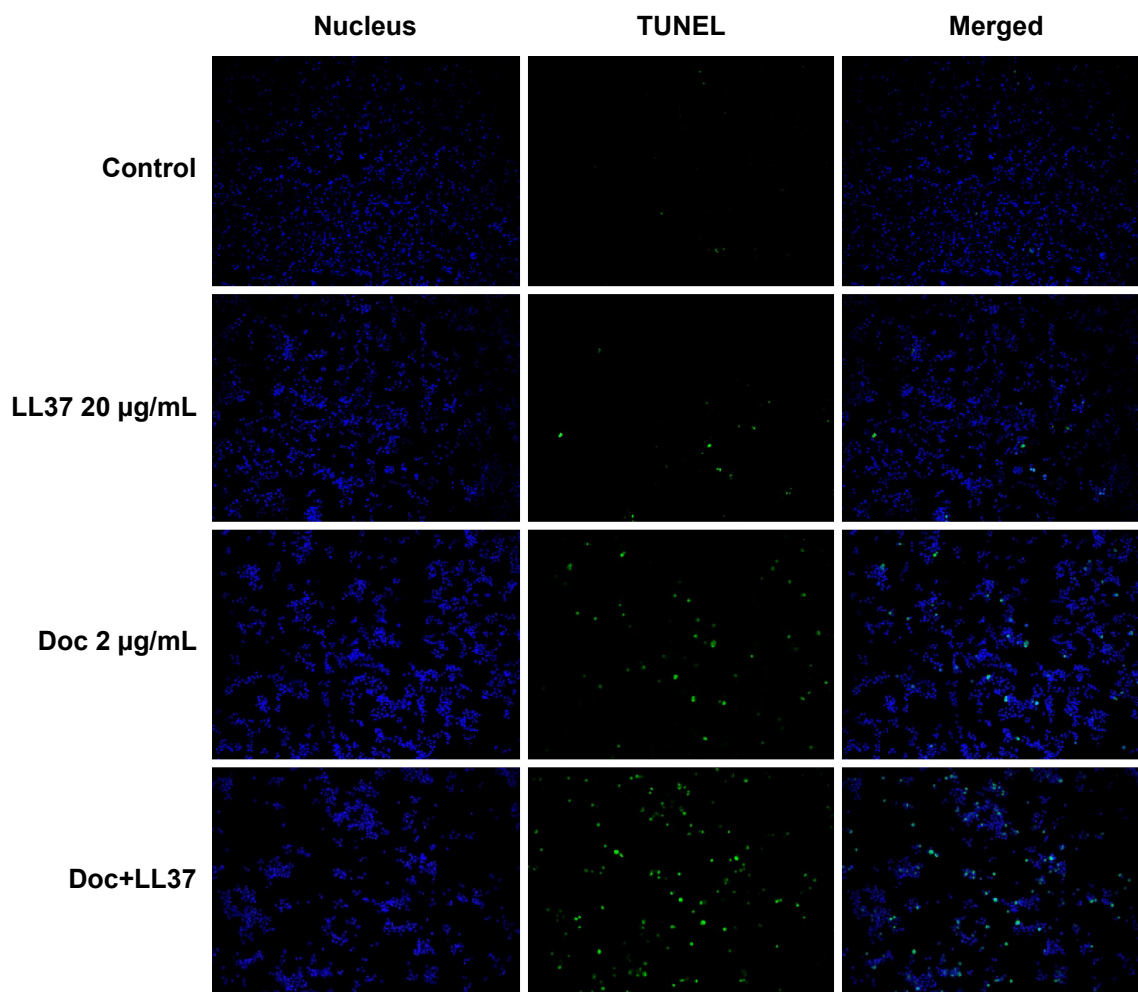


**Figure 7** TUNEL staining confirmed the induction of DNA fragmentation by LL37 (20 µg/mL), Doc (2 µg/mL) and Doc+LL37 (2 µg/mL +20 µg/mL) in HCT116 (24 hours). **Abbreviations:** TUNEL, terminal deoxynucleotidyl transferase deoxyuridine triphosphate nick-end labeling; Doc, docetaxel.

leukemic cell line.<sup>37</sup> However, these studies concentrated on whether LL37, when complexed with self-DNA or DNA vaccine, could promote DNA translocation and may increase the immunostimulatory effects of the self-DNA or DNA vaccine.

Other researchers found that LL37 was substantially downregulated in human colon cancer tissues and could induce apoptosis in cultured colon cancer cells.<sup>1</sup> To test the hypothesis that combination of LL37 and Doc might enhance the antitumor activity of Doc for colorectal peritoneal carcinomatosis, in this study we encapsulated the Doc and LL37 in NPs to prepare combination Doc+LL37 NPs. However, conventional intravenous therapy showed severe systemic toxicity, which remarkably limited the intensity of chemotherapy and diminished the life quality of patients.<sup>38</sup> Thermosensitive hydrogel is an injectable free-flowing sol at ambient temperature, which can instantly convert into a nonflowing gel after injection in vivo. Moreover, intraperitoneal chemotherapy is also a promising postsurgical therapy

of solid carcinomas confined within the peritoneal cavity. Therefore, Doc+LL37 NPs were loaded into PLA-L64-PLA thermosensitive hydrogel to form homogeneous Doc+LL37 NPs-hydrogel composites.

Firstly, a series of PLA-L35-PLA block copolymers were synthesized by ring-opening polymerization. The <sup>1</sup>H-NMR and GPC results indicated that the PLA-L35-PLA block copolymers were prepared successfully with a controlled macromolecular weight. Then, series PLA-L35-PLA block copolymers were used to prepare Doc+LL37 NPs by the w/o/w double-emulsion solvent-evaporation method. Taking the particle size distribution (data not shown) into consideration, the PLA-L35-PLA ( $M_n$  2.0×10<sup>4</sup>, 20 k) was used in the following studies. TEM revealed that the Doc+LL37 NPs formed with the PLA-L35-PLA copolymer were spherical, and the diameters of the NPs observed by TEM were in good agreement with the particle size determined by the Malvern Nano ZS 90 laser particle-size analyzer.

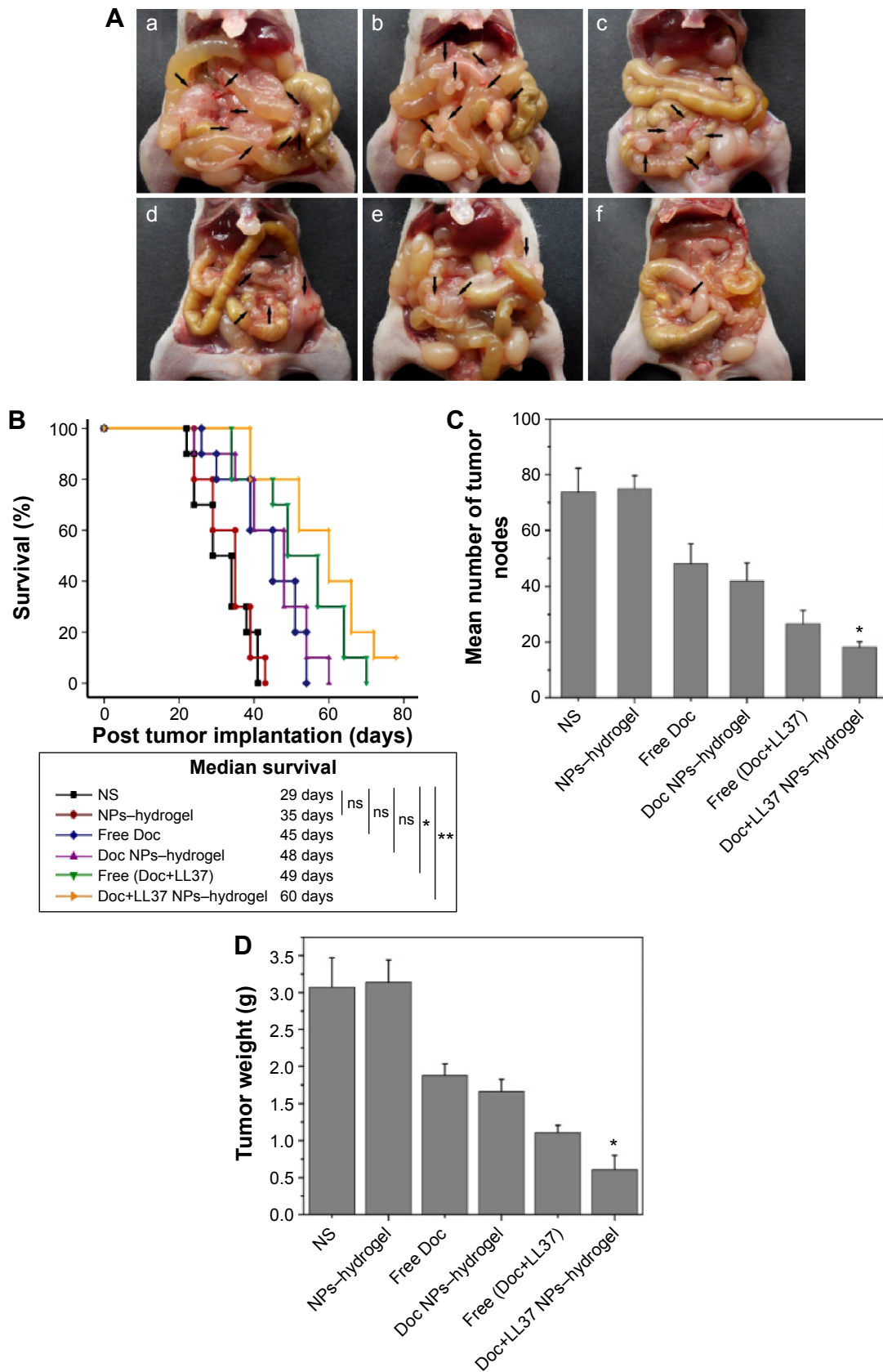


**Figure 8** Intrapertitoneal administration of Doc+LL37 NPs-hydrogel inhibited the growth of abdominal metastases of HCT116 colon carcinoma. **Notes:** Representative photographs of tumors in each group (**A**): normal saline (a), NPs-hydrogel (b), free Doc (c), Doc NPs-hydrogel (d), free Doc+LL37 (e), and Doc+LL37 NPs-hydrogel group (f), the tumor nodules were indicated by the arrows. Kaplan-Meier survival curves of mice in each group (**B**), \* $P < 0.05$  compared to the NS group, and \*\* $P < 0.01$  compared to the NS group. Number of tumor nodules in each group (**C**). Weight of tumor nodules in each group (**D**). **Abbreviations:** Doc, docetaxel; NPs, nanoparticles; NS, normal saline; ns, not significant.

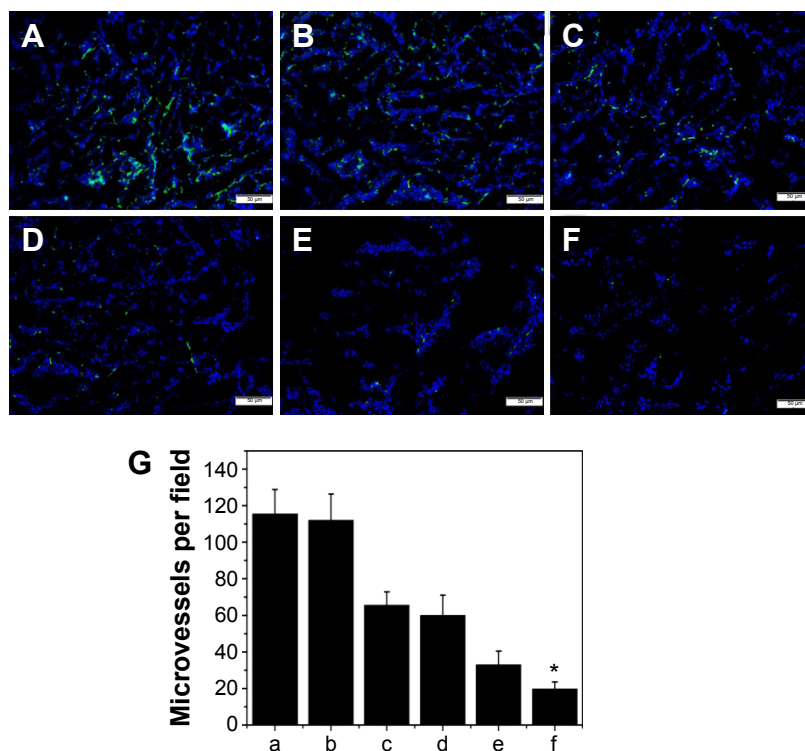


**Figure 9** CD31 immunofluorescent staining of tumors.

**Notes:** Representative CD31 immunofluorescent images of NS (A), NPs–hydrogel (B), free Doc (C), Doc NPs–hydrogel (D), free Doc+LL37 (E), Doc+LL37 NPs–hydrogel group (F), and MVD in each group (G) (a–f corresponding to [A–F], respectively), \* $P < 0.05$  indicates statistically differences from the NS group. Error bars represent standard deviation (n=6).

**Abbreviations:** NS, normal saline; NPs, nanoparticles; Doc, docetaxel; MVD, microvessel density.

In this paper, we developed Doc+LL37 NPs–hydrogel composites that could be injected intraperitoneally and then characterized the composites in detail, and evaluated their anticancer effect *in vivo*. Although the combination of Doc with different agents has been widely studied in the past several years with the final goal of maximizing therapeutic efficacy,<sup>39,40</sup> no studies have to our knowledge reported on the combination of Doc with LL37 for cancer. To evaluate the antitumor effect of combined Doc+LL37 NPs–hydrogel *in vivo*, a murine model of BALB/c nude mice bearing colorectal peritoneal carcinomatosis was used. Doc+LL37 NPs–hydrogel efficiently inhibited the growth of tumors and prolonged the survival of colorectal peritoneal carcinomatosis HCT116-bearing mice. The results of CD31 staining of tumor tissues suggested a potent antiangiogenic effect of the Doc+LL37 NPs–hydrogel composites. In summary, our findings indicate that Doc+LL37 NPs–hydrogel composites may be an ideal treatment for cancer.

## Conclusion

In this work, we prepared a biodegradable and injectable composite to deliver Doc and LL37 for colorectal cancer therapy. The obtained Doc+LL37 NPs–hydrogel composite was an

injectable free-flowing sol at ambient temperature and formed a nonflowing gel at physiological temperature. We demonstrated the advantages of using a Doc+LL37 NPs–hydrogel composite as an anticancer therapeutic approach. The results showed that this composite had promising effects in inhibiting growth of HCT116 colorectal cancer *in vivo*. The mechanisms might involve enhanced apoptosis in tumor cells and suppressed MVD in tumor tissues. The Doc+LL37 NPs–hydrogel composite prepared in this work showed improved antiangiogenesis and antitumor activity, and thus may have potential applications in colorectal carcinoma therapy.

## Acknowledgments

This work was financially supported by the National Natural Sciences Foundation of China (31471286), National S&T Major Project (2011ZX09102-001-10 and 2013ZX09301304-007). The authors deeply appreciate Wang Hui, Wen Jiqui, and Zhu Xiaohong (Analytical and Testing Center, Sichuan University) for their great help on SEM observation, XRD, and FTIR measurement, respectively.

## Disclosure

The authors report no conflicts of interest in this work.

## References

- Ren SX, Cheng AS, To KF, et al. Host immune defense peptide LL-37 activates caspase-independent apoptosis and suppresses colon cancer. *Cancer Res.* 2012;72(24):6512–6523.
- Ren SX, Shen J, Cheng AS, et al. FK-16 derived from the anticancer peptide LL-37 induces caspase-independent apoptosis and autophagic cell death in colon cancer cells. *PLoS One.* 2013;8(5):e63641.
- Yang ZZ, Li JQ, Wang ZZ, Dong DW, Qi XR. Tumor-targeting dual peptides-modified cationic liposomes for delivery of siRNA and docetaxel to gliomas. *Biomaterials.* 2014;35(19):5226–5239.
- Kim DH, Termsarasab U, Cho HJ, et al. Preparation and characterization of self-assembled nanoparticles based on low-molecular-weight heparin and stearylamine conjugates for controlled delivery of docetaxel. *Int J Nanomedicine.* 2014;9:5711–5727.
- Chu KS, Schorzman AN, Finniss MC, et al. Nanoparticle drug loading as a design parameter to improve docetaxel pharmacokinetics and efficacy. *Biomaterials.* 2013;34(33):8424–8429.
- Greco F, Vicent MJ. Combination therapy: opportunities and challenges for polymer-drug conjugates as anticancer nanomedicines. *Adv Drug Deliv Rev.* 2009;61(13):1203–1213.
- Jinturkar KA, Anish C, Kumar MK, Bagchi T, Panda AK, Misra AR. Liposomal formulations of etoposide and docetaxel for p53 mediated enhanced cytotoxicity in lung cancer cell lines. *Biomaterials.* 2012; 33(8):2492–2507.
- Zhou Y, Yang J, Zhang R, Kopeček J. Combination therapy of prostate cancer with HPMA copolymer conjugates containing PI3K/mTOR inhibitor and docetaxel. *Eur J Pharm Biopharm.* 2014;89:107–115.
- Awada A, Albanell J, Canney PA, et al. Bortezomib/docetaxel combination therapy in patients with anthracycline-pretreated advanced/metastatic breast cancer: a phase I/II dose-escalation study. *Br J Cancer.* 2008;98(9):1500–1507.
- Sun L, Zhou DS, Zhang P, Li QH, Liu P. Gemcitabine and  $\gamma$ -cyclodextrin/docetaxel inclusion complex-loaded liposome for highly effective combinational therapy of osteosarcoma. *Int J Pharm.* 2014;478(1):308–317.
- Porcelli F, Verardi R, Shi L, Henzler-Wildman KA, Ramamoorthy A, Veglia G. NMR structure of the cathelicidin-derived human antimicrobial peptide LL-37 in dodecylphosphocholine micelles. *Biochemistry.* 2008;47(20):5565–5572.
- Henzler-Wildman KA, Lee DK, Ramamoorthy A. Mechanism of lipid bilayer disruption by the human antimicrobial peptide, LL-37. *Biochemistry.* 2003;42(21):6545–6558.
- Henzler-Wildman KA, Martinez GV, Brown MF, Ramamoorthy A. Perturbation of the hydrophobic core of lipid bilayers by the human antimicrobial peptide LL-37. *Biochemistry.* 2004;43(26):8459–8469.
- Yan TD, Chu F, Links M, Kam PC, Glenn D, Morris DL. Cytoreductive surgery and perioperative intraperitoneal chemotherapy for peritoneal carcinomatosis from colorectal carcinoma: non-mucinous tumour associated with an improved survival. *Eur J Surg Oncol.* 2006;32(10):1119–1124.
- Hamidi M, Azadi A, Rafiei P. Hydrogel nanoparticles in drug delivery. *Adv Drug Deliv Rev.* 2008;60(15):1638–1649.
- Shimada T, Nomura M, Yokogawa K, et al. Pharmacokinetic advantage of intraperitoneal injection of docetaxel in the treatment for peritoneal dissemination of cancer in mice. *J Pharm Pharmacol.* 2005;57(2):177–181.
- Ozols RF, Bookman MA, Young RC. Intraperitoneal chemotherapy for ovarian cancer. *N Engl J Med.* 2006;354(15):1641–1643.
- Bae WK, Park MS, Lee JH, et al. Docetaxel-loaded thermoresponsive conjugated linoleic acid-incorporated poloxamer hydrogel for the suppression of peritoneal metastasis of gastric cancer. *Biomaterials.* 2013; 34(4):1433–1441.
- Yonemura Y, Endou Y, Bando E, et al. Effect of intraperitoneal administration of docetaxel on peritoneal dissemination of gastric cancer. *Cancer Lett.* 2004;210(2):189–196.
- Kehoe SM, Williams NL, Yakubu R, et al. Incidence of intestinal obstruction following intraperitoneal chemotherapy for ovarian tubal and peritoneal malignancies. *Gynecol Oncol.* 2009;113(2):228–232.
- Nazli C, Ergenc TI, Yar Y, Acar HY, Kizilel S. RGDS-functionalized polyethylene glycol hydrogel-coated magnetic iron oxide nanoparticles enhance specific intracellular uptake by HeLa cells. *Int J Nanomedicine.* 2012;7:1903–1920.
- Fan R, Deng X, Zhou L, et al. Injectable thermosensitive hydrogel composite with surface-functionalized calcium phosphate as raw materials. *Int J Nanomedicine.* 2014;9:615–626.
- Deepa G, Thulasidasan AK, Anto RJ, Pillai JJ, Kumar GS. Cross-linked acrylic hydrogel for the controlled delivery of hydrophobic drugs in cancer therapy. *Int J Nanomedicine.* 2012;7:4077–4088.
- Hoare TR, Kohane DS. Hydrogels in drug delivery: progress and challenges. *Polymer.* 2008;49(8):1993–2007.
- Qiu Y, Park K. Environment-sensitive hydrogels for drug delivery. *Adv Drug Deliv Rev.* 2001;53(3):321–339.
- Irvine DJ. Drug delivery: one nanoparticle, one kill. *Nat Mater.* 2011; 10(5):342–343.
- Brannon-Peppas L, Blanchette JO. Nanoparticle and targeted systems for cancer therapy. *Adv Drug Deliv Rev.* 2004;56(11):1649–1659.
- Singh R, Lillard JW Jr. Nanoparticle-based targeted drug delivery. *Exp Mol Pathol.* 2009;86(3):215–223.
- Tsai M, Lu Z, Wang J, Yeh TK, Wientjes MG, Au JL. Effects of carrier on disposition and antitumor activity of intraperitoneal paclitaxel. *Pharm Res.* 2007;24(9):1691–1701.
- Galaup A, Opolon P, Bouquet C, et al. Combined effects of docetaxel and angiostatin gene therapy in prostate tumor model. *Mol Ther.* 2003; 7(6):731–740.
- Chou TC. Theoretical basis, experimental design, and computerized simulation of synergism and antagonism in drug combination studies. *Pharmacol Rev.* 2006;58(3):621–681.
- Lin BR, Chang CC, Chen RJ, et al. Connective tissue growth factor acts as a therapeutic agent and predictor for peritoneal carcinomatosis of colorectal cancer. *Clin Cancer Res.* 2011;17(10):3077–3088.
- Misra R, Sahoo SK. Coformulation of doxorubicin and curcumin in poly(D,L-lactide-co-glycolide) nanoparticles suppresses the development of multidrug resistance in K562 cells. *Mol Pharm.* 2011;8(3):852–866.
- Yao J, Li Y, Sun X, Dahmani FZ, Liu H, Zhou J. Nanoparticle delivery and combination therapy of gambogic acid and all-trans retinoic acid. *Int J Nanomedicine.* 2014;9:3313–3324.
- Vignoni M, de Alwis Weerasekera H, Simpson MJ, et al. LL37 peptide@silver nanoparticles: combining the best of the two worlds for skin infection control. *Nanoscale.* 2014;6(11):5725–5728.
- Chuang CM, Monie A, Wu A, Mao CP, Hung CF. Treatment with LL-37 peptide enhances antitumor effects induced by CpG oligodeoxynucleotides against ovarian cancer. *Hum Gene Ther.* 2009;20(4):303–313.
- An LL, Yang YH, Ma XT, et al. LL-37 enhances adaptive antitumor immune response in a murine model when genetically fused with M-CSFR (J6-1) DNA vaccine. *Leuk Res.* 2005;29(5):535–543.
- Armstrong DK, Bundy B, Wenzel L, et al. Intraperitoneal cisplatin and paclitaxel in ovarian cancer. *N Engl J Med.* 2006;354(1):34–43.
- Wang L, Zhang M, Zhang N, et al. Synergistic enhancement of cancer therapy using a combination of docetaxel and photothermal ablation induced by single-walled carbon nanotubes. *Int J Nanomedicine.* 2011; 6:2641–2652.
- Conte C, Ungaro F, Maglio G, et al. Biodegradable core-shell nanoassemblies for the delivery of docetaxel and Zn(II)-phthalocyanine inspired by combination therapy for cancer. *J Control Release.* 2013;167(1):40–52.

## Supplementary materials

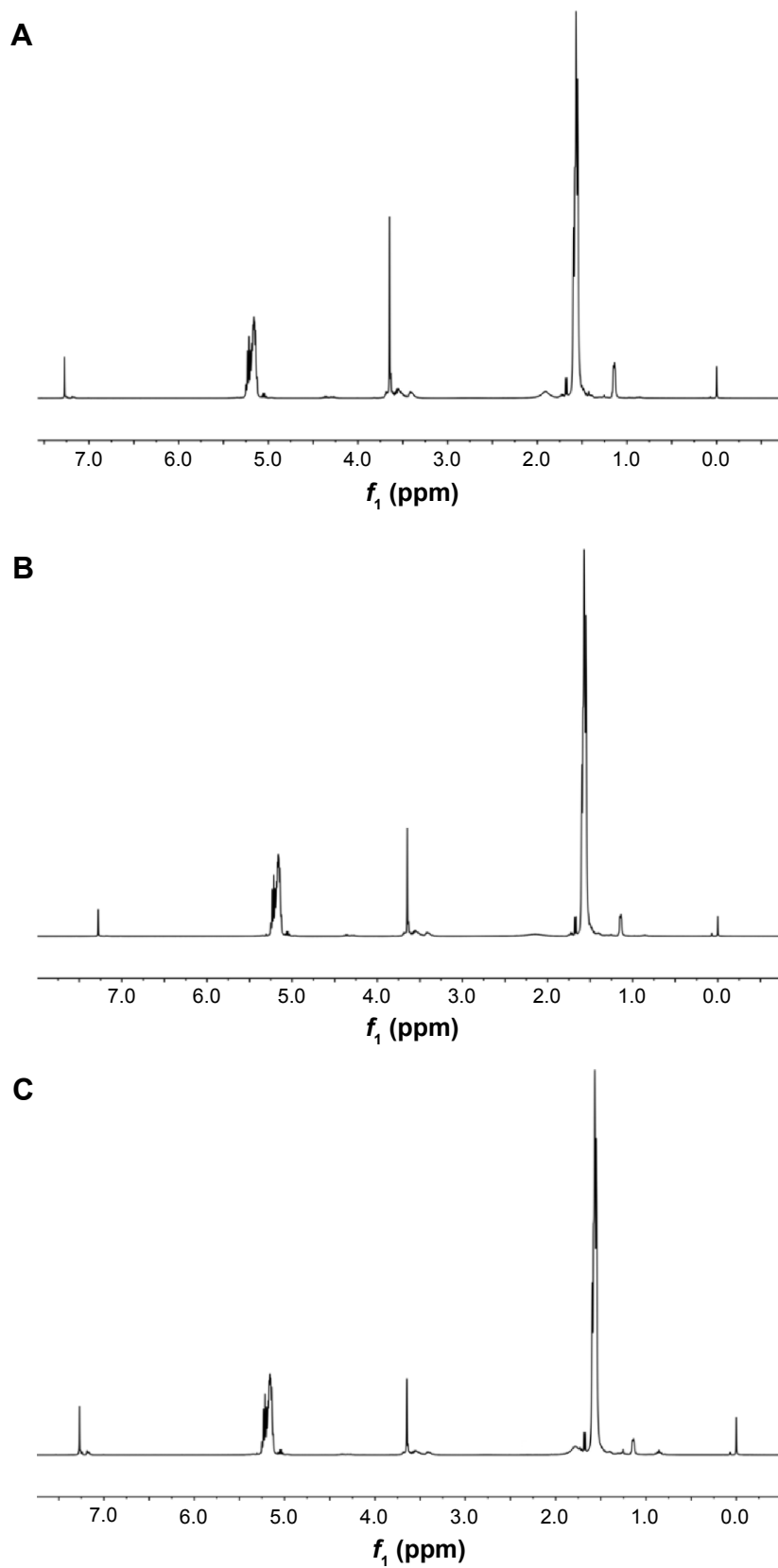


**Figure S1** <sup>1</sup>H-NMR curves of PLA-L35-PLA 10 k (**A**), 20 k (**B**), and 30 k (**C**).

**Abbreviations:** NMR, nuclear magnetic resonance; PLA, polylactic acid; ppm, part per million.

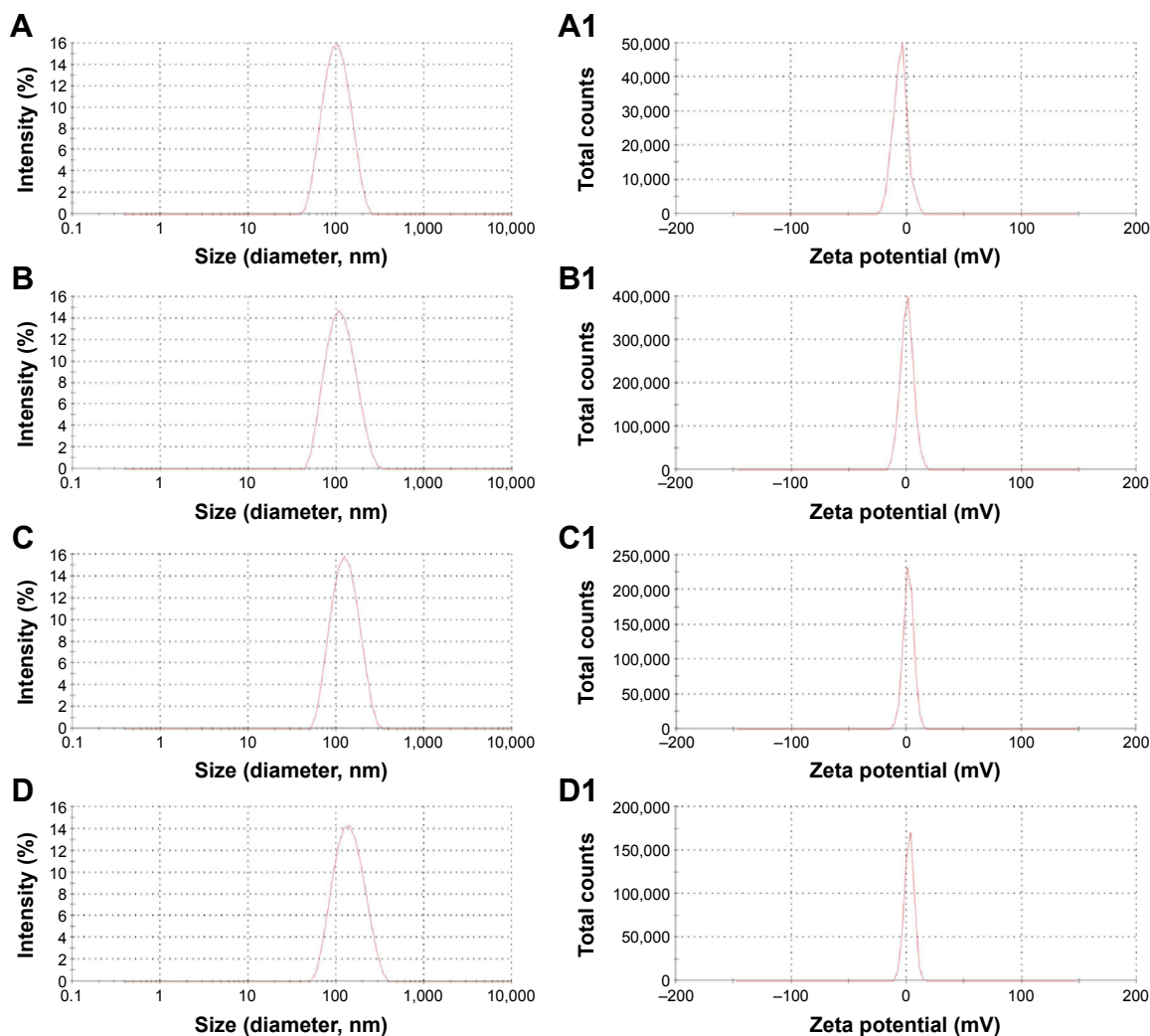


**Figure S2** Particle-size distribution of blank NPs (A), Doc 5%+LL37 2.5% NPs (B), Doc 5%+LL37 5% NPs (C), and Doc 5%+LL37 10% NPs (D). Zeta potential of blank NPs (A1), Doc 5%+LL37 2.5% NPs (B1), Doc 5%+LL37 5% NPs (C1), and Doc 5%+LL37 10% NPs (D1).

**Abbreviations:** NPs, nanoparticles; Doc, docetaxel.

**Table S1** Characterization of Doc+LL37 NPs prepared from PLA-L35-PLA

Sample	PDI	Zeta potential
Blank NPs	0.119±0.019	-5.42±0.12
S1	0.142±0.023	0.51±0.056
S2	0.115±0.021	1.86±0.082
S3	0.125±0.027	2.37±0.08

**Abbreviations:** Doc, docetaxel; NPs, nanoparticles; PLA, polylactic acid; PDI, polydispersity index.

International Journal of Nanomedicine

Publish your work in this journal

The International Journal of Nanomedicine is an international, peer-reviewed journal focusing on the application of nanotechnology in diagnostics, therapeutics, and drug delivery systems throughout the biomedical field. This journal is indexed on PubMed Central, MedLine, CAS, SciSearch®, Current Contents®/Clinical Medicine,

Submit your manuscript here: <http://www.dovepress.com/international-journal-of-nanomedicine-journal>

Dovepress

Journal Citation Reports/Science Edition, EMBase, Scopus and the Elsevier Bibliographic databases. The manuscript management system is completely online and includes a very quick and fair peer-review system, which is all easy to use. Visit <http://www.dovepress.com/testimonials.php> to read real quotes from published authors.